(4)

HIGHER ORDER CROSSINGS FROM A PARAMETRIC FAMILY OF LINEAR FILTERS

Benjamin Kedem and Ta-hsin Li
Department of Mathematics
University of Maryland
College Park, Maryland 20742

August 1989 [1]

MD-89-47-KDM/THL

TR-89-47

[1]Work supported by grants AFOSR-89-0049 and ONR -89-J-1051. The authors wish to thank Woods Hole Oceanographic Institution for the whale data.

SECURITY CLASSIFICATION OF THIS PAGE (When Data Entered)

REPORT DOCUMENTATION PAGE		READ INSTRUCTIONS BEFORE COMPLETING FORM
1. REPORT NUMBER	2. GOVT ACCESSION NO.	3. RECIPIENT'S CATALOG NUMBER
4. TITLE (and Subtitle) Higher order crossings from a parametric family of linear filters		5. TYPE OF REPORT & PERIOD COVERED Technical Report
		6. PERFORMING ORG. REPORT NUMBER
7. AUTHOR(s) Benjamin Kedem and Ta-hsin Li		8. CONTRACT OR GRANT NUMBER(s) ONR N00014-89-J-1051
9. PERFORMING ORGANIZATION NAME AND ADDRESS University of Maryland College Park, MD 20742		10. PROGRAM ELEMENT, PROJECT, TASK AREA & WORK UNIT NUMBERS
11. CONTROLLING OFFICE NAME AND ADDRESS Office of Naval Research Arlington, VA 22217-5000		12. REPORT DATE Sept. 1989
		13. NUMBER OF PAGES 43
14. MONITORING AGENCY NAME & ADDRESS (if different from Controlling Office)		15. SECURITY CLASS. (of this report) Unclassified
		15a. DECLASSIFICATION/DOWNGRADING SCHEDULE

16. DISTRIBUTION STATEMENT (of this Report)

4 copies to Math. Sciences ONR

12 copies to Defense Tech. Inf. Center, Cameron Station, Alexandria, VA 22314

17. DISTRIBUTION STATEMENT (of the abstract entered in Block 20, if different from Report)

18. SUPPLEMENTARY NOTES

19. KEY WORDS (Continue on reverse side if necessary and identify by block number)

Stationary time series, spectrum, Gaussian, HOC-plot, stochastic ordering, sinusoid.

20. ABSTRACT (Continue on reverse side if necessary and identify by block number)

Families and sequences of zero-crossing counts generated by parametric time invariant linear filters are studied. The focus is on the family of zero-crossing counts $\{D_\alpha\}$ generated by the parametric family of filters

$$L_\alpha \equiv 1 + \alpha\beta + \alpha^2\beta^2 + \ldots, \quad \alpha \in (-1,1)$$

where β is the backward shift. In the case of a stationary Gaussian process,

DD FORM 1 JAN 73 1473 EDITION OF 1 NOV 65 IS OBSOLETE

S/N 0102-LF-014-6601

SECURITY CLASSIFICATION OF THIS PAGE (When Data Entered)

20. Abstract (continued)

the expected zero-crossing rate indexed by $\alpha \in (-1,1)$, is always decreasing, completely determines the correlation generating function, and is equal to a constant if and only if the process is a pure sinusoid with probability one. When the process is a sinusoid plus white noise, a sequence $\{E[D_{\alpha_j}], j = 1,2,\ldots\}$ is constructed that after proper normalization converges to the frequency of the sinusoid regardless of the signal to noise ratio. A real data example is given in tracking the vocal sound of a *megaptera novaeangliae* whale.

Abstract

Families and sequences of zero-crossing counts generated by parametric time invariant linear filters are studied. The focus is on the family of zero-crossing counts $\{D_\alpha\}$ generated by the parametric family of filters

$$\mathcal{L}_\alpha \equiv 1 + \alpha\mathcal{B} + \alpha^2\mathcal{B}^2 + \cdots, \alpha \in (-1, 1)$$

where $\mathcal{B}$ is the backward shift. In the case of a stationary Gaussian process, the expected zero-crossing rate indexed by $\alpha \in (-1, 1)$, is always decreasing, completely determines the correlation generating function, and is equal to a constant if and only if the process is a pure sinusoid with probability one. When the process is a sinusoid plus white noise, a sequence $\{E[D_{\alpha_j}], j = 1, 2, \cdots\}$ is constructed that after proper normalization converges to the frequency of the sinusoid regardless of the signal to noise ratio. A real data example is given in tracking the vocal sound of a *megaptera novaeangliae* whale.

<u>**Abbreviated Title:**</u> "Parametric Crossings"

<u>**Key words and phrases:**</u> Stationary time series, spectrum, Gaussian, HOC-plot, stochastic ordering, sinusoid.

<u>**AMS subject classification:**</u> Primary $62M10$, secondary $62M07$.

0.1 Introduction

When a time series is filtered, the effect of the filter can be described by counting the resulting number of zero-crossings. By extension, we can apply to a time series a family of filters and obtain the corresponding family of zero-crossing counts. The resulting family of counts is referred to as *higher order crossings* or HOC. Thus, HOC are zero-crossing counts observed in a time series and in its filtered versions. The main application of HOC is in the description of the oscillation observed in oscillatory time series. Moreover, in the special case of stationary Gaussian time series there are quite a few HOC families and also HOC sequences that determine the spectrum up to a constant.

HOC sequences obtained by repeated differencing have been studied in a sequence of papers beginning with Kedem and Slud (1981, 1982) and reviewed in Kedem(1986). Such HOC are called simple. In this paper we go a step further by introducing the notion of HOC families and sequences obtained from *parametric* time invariant linear filters. The emphasis though is on the useful HOC family obtained from the parametric family of filters

$$\mathcal{L}_\alpha(Z)_t = Z_t + \alpha Z_{t-1} + \alpha^2 Z_{t-2} + \cdots \qquad (0.1)$$

where $\alpha \in (-1,1)$. It is convenient to refer to this filter as the α-filter. It is recognized to be the operation of exponential smoothing. In the Gaussian case, the family of expected HOC obtained by this filter in an α-neighborhood that contains the origin is equivalent to the correlation generating function. Furthermore, the family of expected HOC for $\alpha \in (-1,1)$ is always monotone, a fact that standardizes the application of such HOC in model identification and discrimination between time series. Furthermore, this HOC family contains HOC sequences indexed by $\alpha_j, j = 1,2,\cdots$, that are useful in discrete spectrum estimation in the presence of noise. This is demonstrated in the case of a single frequency when the noise is white Gaussian noise.

In the sequel, by "stationary" we mean both strict and wide sense simultaneously unless we specify an appropriate adjective.

The paper is organized as follows. In section 2 we define and also give examples of HOC from parametric families of linear filters. We outline there our motivation for studying HOC in connection with oscillatory time series.

In section 3 we construct an adaptive HOC sequence from (0.1) that converges to a frequency in the presence of noise. As a matter of fact, the main result there, Corollary 1, has prompted our interest in pursuing HOC in connection with parametric linear operations. In section 4 we obtain more results about the HOC family from (0.1). Our main result there is the connection between the zero-crossing rate, as a function of the parameter, and the correlation generating function under the Gaussian assumption. In section 5 we analyze a vocal sound time series of a ***megaptera novaeangliae*** (humpback) whale.

0.2 Parametric Families of Zero-Crossing Counts

The mathematical formulation of the idea behind HOC can be outlined in four steps as follows.
1. We start with a time series observed in discrete time

$$\{Z_t\},\ t = 0, \pm 1, \pm 2, \cdots$$

2. Let

$$\{\mathcal{L}_\theta(\cdot),\ \theta \in \Theta\}$$

be a parametric family of filters indexed by θ. The parameter space Θ may be an interval or a countable set in one or more dimensions. That is, θ may be a vector.
3. Fix $\theta \in \Theta$ and let D_θ be the number of zero-crossings in discrete time (defined precisely below) observed in the time series

$$\mathcal{L}_\theta(Z)_1, \mathcal{L}_\theta(Z)_2, \cdots, \mathcal{L}_\theta(Z)_N$$

of length N from the filtered process

$$\{\mathcal{L}_\theta(Z)_t\},\ t = 0, \pm 1, \pm 2, \cdots$$

4. The corresponding HOC family is given by

$$\{D_\theta, \theta \in \Theta\}$$

We note that this formulation is somewhat more general in scope than the one given previously in Kedem(1986) and allows for various extensions.

The emphasis in the present paper is on putting together zero-crossing counts and *parametric* linear time invariant filters to produce useful HOC sequences and families. In general, HOC sequences and families contain a great deal of spectral information, and serve as potent features in discrimination and classification. In a more abstract sense, HOC families constitute a combinatorial domain that in many respects is equivalent to the spectral domain and yet this domain has many interesting distinctive features of its own.

Before proceeding with some examples, we must define precisely what is meant by zero-crossing counts in discrete time. For this purpose it is convenient to introduce the family of binary time series:

$$X_t(\theta) = \begin{cases} 1, & \text{if } \mathcal{L}_\theta(Z)_t \geq 0 \\ 0, & \text{if } \mathcal{L}_\theta(Z)_t < 0 \end{cases}$$

$t = 0, \pm 1, \pm 2, \cdots$ The number of zero-crossings in $\mathcal{L}_\theta(Z)_1, \mathcal{L}_\theta(Z)_2, \cdots, \mathcal{L}_\theta(Z)_N$ is defined as the number of symbol changes in $X_1(\theta), \cdots, X_N(\theta)$:

$$D_\theta = \sum_{t=2}^{N} [X_t(\theta) - X_{t-1}(\theta)]^2$$

When, for some θ, $\mathcal{L}_\theta(\cdot)$ corresponds to the identity filter then D_θ is the number of zero-crossings in the original unfiltered series $Z_1, \cdots, Z_N$. We can see that D_θ depends on N and that this dependence is more apparent in the zero-crossing rate defined by

$$\gamma_N(\theta) \equiv \frac{D_\theta}{N-1}$$

But, clearly, the expected rate

$$\gamma(\theta) \equiv \frac{E[D_\theta]}{N-1}$$

need not depend on N as is the case for a strictly stationary process. In studying HOC families, at times we let θ change while holding N fixed and at other times θ is fixed but N changes.

0.2.1 Examples of Parametric HOC Families

(1). HOC from differences.

Let ∇ be the difference operator defined by

$$\nabla Z_t \equiv Z_t - Z_{t-1}$$

and define

$$\mathcal{L}_\theta \equiv \nabla^{\theta-1}, \theta \in \{1, 2, 3, \cdots\}$$

with $\mathcal{L}_1 \equiv \nabla^0$ being the identity filter. The corresponding HOC sequence

$$D_1, D_2, D_3, \cdots$$

gives the simple HOC. When Z_t is a zero-mean stationary Gaussian process with spectral distribution function $F(\omega)$ then, by virtue of the well known *arcsine-law* (e.g. David (1953)), the simple HOC obtained by repeated differencing admit the spectral representation (Kedem(1986))

$$\rho_1(\theta) = cos[\pi\gamma(\theta)] = \frac{\int_{-\pi}^{\pi} cos(\omega)(sin(\omega/2))^{2(\theta-1)} dF(\omega)}{\int_{-\pi}^{\pi} (sin(\omega/2))^{2(\theta-1)} dF(\omega)} \tag{0.2}$$

where $\rho_1(\theta)$ is the first-order correlation in the filtered process $\{\mathcal{L}_\theta(Z)_t\}$. The sequence $\gamma(\theta)$ is bounded and monotone increasing in θ so that

$$\pi\gamma(\theta) \longrightarrow \omega^*, \ \theta \longrightarrow \infty \tag{0.3}$$

where ω^* is the highest frequency in the spectral support. We shall provide a proof of this fact later. When $\gamma(1) = \gamma(2)$ then Z_t is a pure sinusoid and $\pi\gamma(\theta)$ is a constant equal to the frequency of the sinusoid (Kedem(1984)).

It should be noted that in the Gaussian case the left hand side of (0.2), $\rho_1(\theta) = cos[\pi\gamma(\theta)]$, *holds in general for any filtered process* $\{\mathcal{L}_\theta(Z)_t\}$. *This "cosine-formula" is known to hold also for processes whose finite dimensional distributions are spherically symmetric of which the Gaussian distribution is a special case (He and Kedem (1988)). The formula is of fundamental importance in the study of HOC, and finding a similar formula for stationary processes whose finite dimensional distributions are not spherically symmetric is a challanging and intriguing problem.*

(2). HOC from repeated summation.
Let $\mathcal{B}$ be the shift operator defined by

$$\mathcal{B}Z_t = Z_{t-1}$$

and define

$$\mathcal{L}_\theta \equiv (1 + \mathcal{B})^{\theta-1}, \ \theta \in \{1, 2, 3, \cdots\}$$

The corresponding HOC are called HOC from repeated summation and the sequence $\{D_\theta\}$ is monotone decreasing in θ, and in the Gaussian case

$$\pi\gamma(\theta) \longrightarrow \omega_*, \ \theta \longrightarrow \infty \tag{0.4}$$

where ω_* is the lowest frequency in the spectral support of $F(\omega)$. This can be shown using the spectral representation

$$cos[\pi\gamma(\theta)] = \frac{\int_{-\pi}^{\pi} cos(\omega)(1+cos(\omega))^{(\theta-1)}dF(\omega)}{\int_{-\pi}^{\pi}(1+cos(\omega))^{(\theta-1)}dF(\omega)} \tag{0.5}$$

From (0.3) and (0.4) we can determine all the frequencies and their number in a stationary Gaussian process with a purely discrete spectrum. First, from (0.4), we obtain the lowest frequency by repeated summation. Then, from (0.3), we obtain the highest frequency and filter it out, the second highest and filter it out, and so on until there is a single frequency left in which case it must be the lowest one that we already know, and we stop (Kedem(1986)).

(3). HOC from exponential smoothing.
We can rewrite (0.1) more compactly as follows. Let

$$Z_t(\alpha) \equiv \mathcal{L}_\alpha(Z)_t$$

Then (0.1) becomes

$$Z_t(\alpha) = \alpha Z_{t-1}(\alpha) + Z_t, \ \alpha \in (-1,1) \tag{0.6}$$

The corresponding HOC family $\{D_\alpha\}$, $\alpha \in (-1,1)$ is the main subject of the present paper. When $\{Z_t\}$ is a zero mean stationary Gaussian process then, as we shall see, $\gamma(\alpha)$ is monotone decreasing, and we obtain the spectral representation

$$cos[\pi\gamma(\alpha)] = \frac{\int_{-\pi}^{\pi} cos(\omega)|H(\omega;\alpha)|^2dF(\omega)}{\int_{-\pi}^{\pi}|H(\omega;\alpha)|^2dF(\omega)} \tag{0.7}$$

where

$$|H(\omega;\alpha)|^2 = \frac{1}{1-2\alpha cos(\omega)+\alpha^2}, \ \ \alpha \in (-1,1), \ \omega \in [0,\pi] \tag{0.8}$$

In that case we show that $\gamma(\alpha)$ is equivalent to the normalized spectrum. In general, however, this equivalence need not hold and $\gamma(\alpha)$ may contain some extra useful information. This point is brought up again later in a real data example where we apply both the spectral density and $\gamma_N(\alpha)$ in the analysis of vocal sound of a humpback whale.

(4). HOC from autoregressive moving averages operations.
A more general family of parametric filters, and one that contains the previous examples as special cases, is defined by the autoregressive-moving average operation

$$Y_t - a_1 Y_{t-1} - \cdots - a_p Y_{t-p} = Z_t - b_1 Z_{t-1} - \cdots b_q Z_{t-q} \tag{0.9}$$

where now

$$D_\theta \equiv D_{a_1,a_2,\cdots,b_1,b_2,\cdots}$$

Not much is known at present about the HOC $\{D_\theta\}$ of this general case, except for some results of a general nature given below.

0.2.2 HOC-plots from a process with adjoined random variables.

To illustrate the ability of HOC to summarize and describe the oscillation in time series, it is instructive to consider some special cases while exploiting the strong graphical appeal inherent in HOC. For this purpose we consider a zero-mean non-Gaussian stationary process defined as follows. Let

$$T_1, T_2, T_3, \cdots$$

be a sequence of IID random variables from a geometric distribution with parameter p, and let

$$U_1, U_2, U_3, \cdots$$

be a sequence of independent standard normal random variables. Consider the stationary process $\{Z_t\}$ defined by:

$$\begin{aligned} Z_t &= U_1, \quad 1 \le t \le T_1 \\ Z_t &= U_2, \quad T_1 < t \le T_2 \end{aligned}$$

$$Z_t = U_3, \quad T_2 < t \le T_3$$

$$\vdots$$

The process $\{Z_t\}$ is called a process with adjoined random variables. Its behavior is determined by the parameter p. Figure 1 shows realizations of the process corresponding to $p = 0.10, 0.25, 0.50, 0.75$. The corresponding normalized HOC plots of $\gamma_N(\cdot)$ from simple HOC and HOC obtained from the α-filter (0.1) are given in Figure 2. The figures also contain the normalized HOC $\gamma_N(\cdot)$ from white Gaussian noise for the sake of comparison. We see that simple HOC increase while the HOC from the α-filter decrease as they should. The reason for this displayed monotonicity is that the gain functions of these parametric linear filters are themselves monotone. See Theorem 2 below.

Figure 1. Realizations from processes with adjoined random variables with p=0.1, 0.25, 0.5, 0.75.

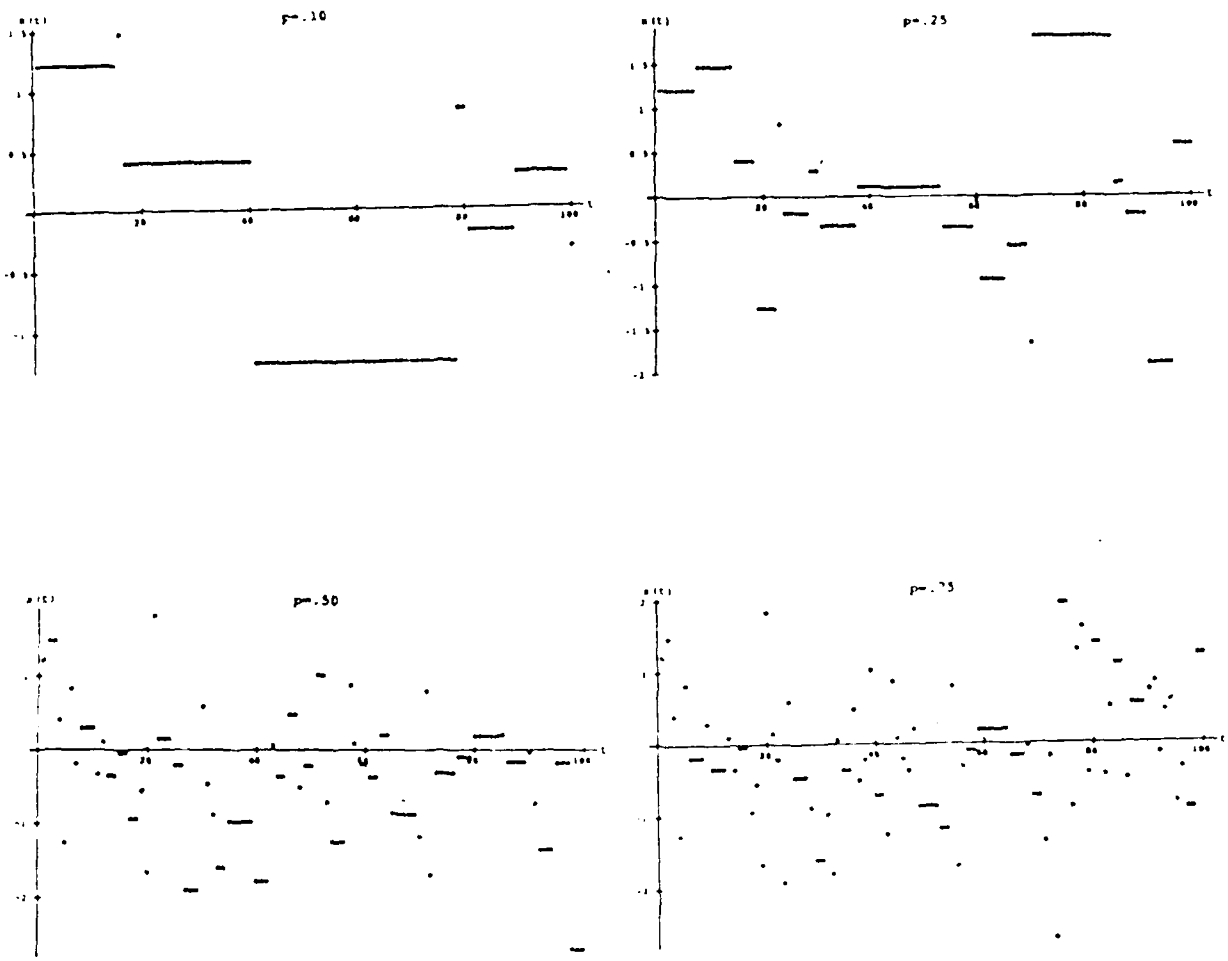

Figure 2. Plots of normalized HOC. (a) Simple HOC. (b) HOC from the α-filter.

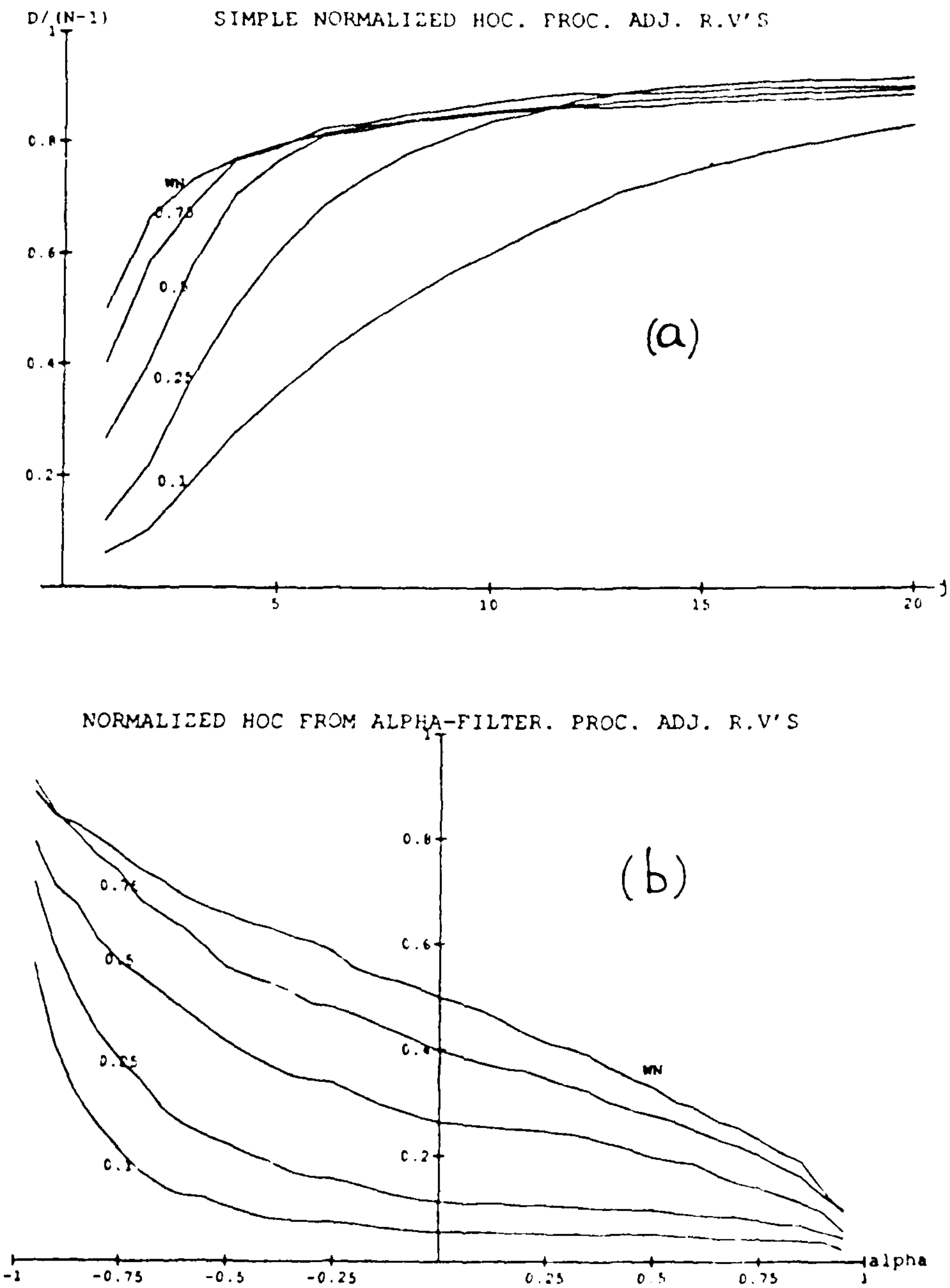

0.2.3 Why HOC ?

There is a close association between the autocorrelation function ρ_k and HOC. As remarked earlier, in the Gaussian case, there are HOC families that are equivalent to the autocorrelation. For example, knowledge of the sequence of expected HOC from differencing $E[D_j]$ is equivalent to knowing ρ_k in the sense that each sequence completely determines the other. Thus it seems tempting to say, at least when facing that equivalence, that the close association between HOC and ρ_k eliminates the need for HOC. The truth, however, is that HOC sequences and families have certain inherent advantages over the autocorrelation that warrant their study. Here are some.

(1). Resistance to outliers.
In the presence of extreme values, the sample auotocorrelation may resemble the auotocorrelation of white noise. This can easily be seen when a time series contains a single large outlier. In this case the sample auotocorrelation tends to zero. The zero-crossing count from the unfiltered original data however is left intact. The same also holds after decimation when only subseries (e.g. $Z_1, Z_3, Z_5, \cdots$) are considered.

(2). Relation to the spectral support.
The normalized quantity

$$\pi\gamma(\theta) \equiv \frac{\pi E[D_\theta]}{N-1}$$

takes values in the interval $[0, \pi]$. It is therefore easy to relate it directly to specific frequency bands and discrete frequencies in the spectral support. When θ corresponds to a highpass (lowpass) filter, $\pi\gamma(\theta)$ moves to the right (left) so that by varying θ intelligently we can force or "push" $\pi\gamma(\theta)$ to land on any desired frequency. Important special cases of this fact were already seen earlier in (0.3), (0.4), and are seen again later in Theorem 1 and its corollary.

It is interesting to observe that the point $\pi\gamma(\theta)$ can be moved along the spectral support by adding sinusoidal components at will. High (low) frequency components with sufficient power can cause $\pi\gamma(\theta)$ to move to the right (left) as is the case with highpass (lowpass) filtering.

(3). Exceeding autocorrelation information.

For *non-Gaussian* processes $\{D_\theta, \theta \in \Theta\}$ may contain more information than the autocorrelation. As alluded to earlier, a clear indication of this fact is given in our data example in section 5. In general, $\{D_\theta, \theta \in \Theta\}$ may be interpreted as yet another type of "spectrum" that relates directly to oscillation. In this respect $\pi D_\theta/(N-1)$, where θ corresponds to the identity operation, may be viewed as the basic "period" of the process.

(4). Graphical information.

HOC sequences and families convey a great deal of graphical information that can be related to the general appearance of time series. For example, simple HOC from differencing $D_1, D_2, D_3, \cdots$, pertain to zero-crossings, peaks and troughs, inflection points, $\cdots$, respectively. In this connection it is worth noting that if $D_j \approx D_{j+1}$ for *low* order j, then there is good chance the data contains a marked sinusoidal component.

(5). Lack of moments.

A strictly stationary process may not possess moments of any order so that the usual definition of autocorrelation and spectrum does not apply. HOC, however, adapt easily to this situation because

$$\pi\gamma_N(\theta) \equiv \frac{\pi D_\theta}{N-1}$$

possesses all moments. Thus HOC can provide a first hand feel of the oscillation regardless of the existence of moments.

(6). Lack of stationarity.

A non stationary process may still generate very regular oscillation despite of its overall time dependent behavior. When this is the case, the zero-crossing rate is a quantity to be reckoned with. An example is furnished by a nonstationary AR(2) with two unit roots $exp(\pm\zeta)$. The process is both explosive and also very oscillatory, but its oscillation is essentially the same as that of a pure sinusoid. It has been shown in He and Kedem (1989*b*) that

$$l.i.m._{N\longrightarrow\infty}\frac{\pi D_1}{N-1} = \zeta, \quad 0 \le \zeta \le \pi$$

where D_1 is the number of zero-crossings in the observed unfiltered time series. Note that this is an example where $\theta = 1$ is fixed while N changes.

0.3 Detection of a single frequency in noise.

The ideas expressed above can be illustrated very well by considering the problem of detecting a single frequency in the presence of white Gaussian noise using the α-filter. We shall construct an expected *HOC* sequence that, under the Gaussian assumption, converges to the frequency regardless of the magnitude of the noise variance. For this purpose we generalize a result of He and Kedem (1989*a*).

First we need

Lemma 1. Let $|H(\omega;\alpha)|^2$ be given by (0.8), and let p be a positive integer. For

$$0 < \omega_1 < \omega_2 < \cdots < \omega_p \leq \pi$$

and for positive constatnts

$$\sigma_1^2, \sigma_2^2 \cdots, \sigma_p^2$$

define the convex combination

$$\xi(\alpha) = \frac{\sum_{j=1}^{p} \sigma_j^2 |H(\omega_j;\alpha)|^2 cos(\omega_j)}{\sum_{j=1}^{p} \sigma_j^2 |H(\omega_j;\alpha)|^2} \tag{0.10}$$

Then $\xi(\alpha)$ is monotone increasing for $\alpha \in (-1,1)$.

Proof: For $\alpha_1, \alpha_2 \in (-1,1)$ suppose $\alpha_1 \leq \alpha_2$, and define

$$a_{kl} \equiv |H(\omega_k;\alpha_1)|^2 |H(\omega_l;\alpha_2)|^2$$

for $k,l,= 1,\cdots,p$. To show that $\xi(\alpha_2) - \xi(\alpha_1) \geq 0$ it is sufficient to show that for any choice of $k < l$, $a_{lk} - a_{kl} \geq 0$ where $\omega_k \leq \omega_l$, or equivalently, $cos(\omega_k) \geq cos(\omega_l)$. The numerator of $a_{lk} - a_{kl}$ is equal to

$$2(cos(\omega_k) - cos(\omega_l))(1 - \alpha_1\alpha_2)(\alpha_2 - \alpha_1) \geq 0$$

The corresponding denominator is always positive, and the lemma is proved. □

Consider now the mixed spectrum stationary Gaussian process

$$Z_t = \sum_{j=1}^{p} (A_j cos(\omega_j t) + B_j sin(\omega_j t)) + \epsilon_t \tag{0.11}$$

where the A's and B's are all independent, $A_j, B_j \sim N(0, \sigma_j^2)$, and $\{\epsilon_t\}$ is white Gaussian noise with mean 0 and variance σ_ϵ^2, independent of the A's and B's. As before $0 < \omega_1 < \omega_2 < \cdots < \omega_p \leq \pi$. We have

Theorem 1. Consider the harmonic process (0.11) and choose an arbitrary constant $\alpha_0 \in (-1, 1)$. Define the sequence

$$\alpha_{j+1} = cos(\frac{\pi E[D_{\alpha_j}]}{N-1}) \tag{0.12}$$

Then as $j \to \infty$

$$\alpha_j \to \alpha^*$$

where α^* is a fixed point solution of the equation

$$\xi(\alpha^*) = \alpha^* \tag{0.13}$$

and

$$\omega_1 \leq \frac{\pi E[D_{\alpha^*}]}{N-1} \leq \omega_p$$

Proof: Let $|H(\omega;\alpha)|^2$ be given by (0.8). The Gaussian assumption implies that

$$cos(\frac{\pi E[D_\alpha]}{N-1}) = \frac{\int_0^\pi cos(\omega)|H(\omega;\alpha)|^2 dF(\omega)}{\int_0^\pi |H(\omega;\alpha)|^2 dF(\omega)} \tag{0.14}$$

where $F(\omega)$ is the spectral distribution function of $\{Z_t\}$. Define

$$W(\alpha) = \frac{\sigma_\epsilon^2}{\pi} \frac{\int_0^\pi |H(\omega;\alpha)|^2 d\omega}{\sum_{j=1}^p \sigma_j^2 |H(\omega_j;\alpha)|^2} \tag{0.15}$$

Then from (12), (14), (15) it follows that for $k = 0, 1, 2, \cdots$

$$\alpha_{k+1} = \frac{\xi(\alpha_k) + W(\alpha_k)\alpha_k}{1 + W(\alpha_k)} \tag{0.16}$$

In deriving (0.16) it helps to observe that

$$\int_0^\pi |H(\omega;\alpha)|^2 d\omega = \frac{\pi}{1-\alpha^2}$$

and

$$\int_0^{\pi} cos(\omega)|H(\omega;\alpha)|^2 d\omega = \frac{\pi}{1-\alpha^2}\alpha$$

Observe that α_{k+1} is a convex combination and that it must fall between α_k and $\xi(\alpha_k)$. Suppose $\alpha_0 \leq \xi(\alpha_0)$. Then

$$\alpha_0 \leq \alpha_1 \leq \xi(\alpha_0)$$

But $\xi(\alpha)$ is monotone increasing so that

$$\alpha_0 \leq \alpha_1 \leq \xi(\alpha_1)$$

Similarly, whenever $\alpha_j \leq \alpha_{j+1} \leq \xi(\alpha_{j+1})$ then

$$\alpha_{j+1} \leq \alpha_{j+2} \leq \xi(\alpha_{j+2})$$

and so $\{\alpha_j\}$ is a monotone sequence. But for $\alpha \in (-1,1)$

$$cos(\omega_p) \leq \xi(\alpha) \leq cos(\omega_1)$$

and therefore $\{\alpha_j\}$ is also bounded. It follows that $\{\alpha_j\}$ converges to α_*, say. Then from (0.16)

$$\alpha_* = \frac{\xi(\alpha_*) + W(\alpha_*)\alpha_*}{1 + W(\alpha_*)} \tag{0.17}$$

or that

$$\alpha_* = \xi(\alpha_*)$$

Conversely, suppose $\alpha_0 \geq \xi(\alpha_0)$. Then by a similar argument there exists an α_{**} such that $\alpha_j \to \alpha_{**}$ and

$$\alpha_{**} = \xi(\alpha_{**})$$

It follows that as $j \to \infty$, $\alpha_j \to \alpha^*$, where $\alpha^* = \xi(\alpha^*)$ for some

$$\alpha^* \in (cos(\omega_p), (cos(\omega_1))$$

or equivalently

$$\frac{\pi E[D_{\alpha_j}]}{N-1} \to \frac{\pi E[D_{\alpha^*}]}{N-1} \in (\omega_1, \omega_p)$$

□

For the case $p = 1$ we obtain the result of He and Kedem (1989a).

Corollary 1. Suppose $p = 1$. Then regardless of the signal to noise ratio,

$$\frac{\pi E[D_{\alpha_j}]}{N-1} \rightarrow \omega_1, \quad j \rightarrow \infty \tag{0.18}$$

Proof: Here $\omega_p = \omega_1$. □

Table 1 shows some examples of the convergence in (0.18) using simulated data of a single sinusoid plus noise. In applications $\gamma(\alpha)$ is replaced by $\gamma_N(\alpha)$, a consistent estimate under the model at hand. Evidently, for reasonable signal to noise ratio the algorithm converges rather fast. Observe that no Fourier type analysis has been used, and that ω_1 need not be a Fourier frequency of the form $2\pi k/N$.

Table 1. Convergence of $\frac{\pi D_{\alpha_J}}{N-1}$ towards $\omega_1 = 0.8$ with $N = 10000$ where the signal to noise ratio (SNR) is given in dB.

1dB $\alpha_0 = -.1$	0dB $\alpha_0 = .9$	-1.94dB $\alpha_0 = .2$	-6.02dB $\alpha_0 = .5$	-10dB $\alpha_0 = .1$
0.8848	0.5194	0.9127	0.9291	1.3381
0.8006	0.5904	0.8222	0.8713	1.2294
0.7987	0.6563	0.8015	0.8411	1.1251
0.7987	0.7142	0.7965	0.8191	1.0371
0.7987	0.7600	0.7952	0.8053	0.9617
0.7987	0.7864	0.7952	0.8015	0.9077
0.7987	0.8002	0.7952	0.7990	0.8756
0.7987	0.8065	0.7952	0.7984	0.8511
0.7987	0.8065	0.7952	0.7977	0.8449
0.7987	0.8065	0.7952	0.7971	0.8436
0.7987	0.8065	0.7952	0.7971	0.8423
0.7987	0.8065	0.7952	0.7971	0.8405
0.7987	0.8065	0.7952	0.7971	0.8392
0.7987	0.8065	0.7952	0.7971	0.8379
0.7987	0.8065	0.7952	0.7971	0.8361
0.7987	0.8065	0.7952	0.7971	0.8335
0.7987	0.8065	0.7952	0.7971	0.8323
0.7987	0.8065	0.7952	0.7971	0.8310
0.7987	0.8065	0.7952	0.7971	0.8298
0.7987	0.8065	0.7952	0.7971	0.8310
0.7987	0.8065	0.7952	0.7971	0.8298
.	.	.	.	.
.	.	.	.	.
.	.	.	.	.

<u>Note:</u> $SNR \equiv 20 log_{10} \frac{s.d.signal}{s.d.noise} \; dB$

0.4 The HOC from the α-filter

In the previous section we were concerned with an important special case of spectrum analysis. It was shown that the HOC family from the α-filter contains a sequence that (after proper normalization) converges to a discrete frequency amidst white noise. This fact emboldens us to believe that the HOC from the α-family contains considerably more spectral information. That this is indeed the case is shown in the present section. It is shown that in the Gaussian case the HOC family from the α-filter completely determines the correlation generating function of the original unfiltered process.

0.4.1 Preliminary results on linear filtering

Let $\{Z_t\}, t = 0, \pm 1, \pm 2 \cdots$, be a zero mean stationary process with autocovariance R_k, autocorrelation ρ_k, and generalized spectral density $f(\omega)$ that contains δ-functions correspinding to the points of jump in the spectral distribution function. Let $\mathcal{L}_\alpha$ be a parametric family of linear time invariant filters with impulse response $\{h_n(\alpha)\}_{-\infty}^{\infty}$ and transfer function $H(\omega;\alpha)$ where

$$H(\omega;\alpha) \equiv \mathcal{FT}(h_n(\alpha)) = \sum_n \exp(-in\omega)h_n(\alpha) \tag{0.19}$$

Wherever applicable, we always make the regularity assumptions that $h_n(\alpha)$ is absolutely summable in n and that

$$\int_{-\pi}^{\pi} |H(\omega;\alpha)|^2 f(\omega)d\omega < \infty \tag{0.20}$$

We define the filtered process indexed by α as before

$$Z_t(\alpha) \equiv \mathcal{L}_\alpha(Z)_t = \sum_n h_n(\alpha)Z_{t-n} \tag{0.21}$$

In other words

$$Z_t(\alpha) \equiv h_t(\alpha) \otimes Z_t \tag{0.22}$$

where $\otimes$ denotes convolution. Denote the autocovariance and autocorrelation of $\{Z_t(\alpha)\}$ by $R_k(\alpha)$, and $\rho_k(\alpha)$, respectively.

The next result shows how to compute the autocorrelation of $\{Z_t(\alpha)\}$ from ρ_k . The result is well known but it is brought here for completeness.

Lemma 2. Let $\mathcal{J}_\alpha$ be a time invariant linear filter, indexed by α, whose impulse response $\{g_n(\alpha)\}_{-\infty}^{\infty}$ is given by the convolution

$$g_n(\alpha) = h_n(\alpha) \otimes h_{-n}(\alpha)$$

Then

$$\rho_n(\alpha) = \frac{\mathcal{J}_\alpha(\rho)_n}{\mathcal{J}_\alpha(\rho)_0} \tag{0.23}$$

and

$$\mathcal{J}_\alpha(\rho)_n = g_n(\alpha) + \sum_{t=1}^{\infty}(g_{n+t}(\alpha) + g_{n-t}(\alpha))\rho_t, \tag{0.24}$$

$$n = 0, \pm 1, \pm 2, \cdots \tag{0.25}$$

Proof: Observe that

$$\mathcal{FT}(\mathcal{J}_\alpha(R)_n) = \mathcal{FT}(g_n(\alpha) \otimes R_n) = \mathcal{FT}(h_n(\alpha) \otimes h_{-n}(\alpha) \otimes R_n) = H(\omega;\alpha)\overline{H(\omega;\alpha)}2\pi f(\omega)$$

By taking the inverse Fourier transform we obtain

$$\mathcal{J}_\alpha(R)_n = \int_{-\pi}^{\pi} \exp(in\omega)|H(\omega;\alpha)|^2 f(\omega)d\omega = R_n(\alpha)$$

Therefore

$$\rho_n(\alpha) = \frac{R_n(\alpha)}{R_0(\alpha)} = \frac{\mathcal{J}_\alpha(R)_n}{\mathcal{J}_\alpha(R)_0} = \frac{R_0\mathcal{J}_\alpha(\rho)_n}{R_0\mathcal{J}_\alpha(\rho)_0}$$

□

An important consequence of the application of a linear filter is that the autocorrelation is altered. In particular if in addition the gain function is monotone increasing (decreasing) the process becomes more (less) oscillatory and the correlation between neighboring points decreases (increases). Intuitively this is what one expects of highpass (lowpass) filtering, but in the case of monotone gains this intuition becomes factual as shown in the following theorem.

Theorem 2. Suppose the squared gain function $|H(\omega)|^2$ is monotone increasing in $[0,\pi]$. Denote by $\rho_1(H)$ the first-order correlation in the filtered process. Then

$$\rho_1 \geq \rho_1(H) \tag{0.26}$$

When the gain is monotone decreasing the inequality is reversed.

Proof: The proof makes use of properties of stochastic ordering. Define for $\lambda \in [0,\pi]$ the *probability* distribution functions,

$$\tilde{F}(\lambda) \equiv \frac{\int_0^\lambda f(\omega)d\omega}{\int_0^\pi f(\omega)d\omega}$$

and

$$\tilde{F}_H(\lambda) \equiv \frac{\int_0^\lambda |H(\omega)|^2 f(\omega)d\omega}{\int_0^\pi |H(\omega)|^2 f(\omega)d\omega}$$

Suppose $|H(\omega)|^2$ is monotone increasing. Then

$$\begin{aligned}
&\tilde{F}(\lambda) - \tilde{F}_H(\lambda) \\
&= \frac{\int_0^\pi |H(\omega)|^2 f(\omega)d\omega \int_0^\lambda f(\omega)d\omega - \int_0^\pi f(\omega)d\omega \int_0^\lambda |H(\omega)|^2 f(\omega)d\omega}{\int_0^\pi f(\omega)d\omega \int_0^\pi |H(\omega)|^2 f(\omega)d\omega} \\
&= \frac{\int_\lambda^\pi |H(\omega)|^2 f(\omega)d\omega \int_0^\lambda f(\omega)d\omega - \int_\lambda^\pi f(\omega)d\omega \int_0^\lambda |H(\omega)|^2 f(\omega)d\omega}{\int_0^\pi f(\omega)d\omega \int_0^\pi |H(\omega)|^2 f(\omega)d\omega} \\
&\geq \frac{|H(\lambda)|^2 \int_\lambda^\pi f(\omega)d\omega \int_0^\lambda f(\omega)d\omega - |H(\lambda)|^2 \int_\lambda^\pi f(\omega)d\omega \int_0^\lambda f(\omega)d\omega}{\int_0^\pi f(\omega)d\omega \int_0^\pi |H(\omega)|^2 f(\omega)d\omega} \\
&= 0
\end{aligned}$$

and therefore for all $\lambda \in [0,\pi]$

$$\tilde{F}(\lambda) \geq \tilde{F}_H(\lambda) \tag{0.27}$$

Thus, if X, Y are two random variables such that

$$X \sim \tilde{F}_H, \quad Y \sim \tilde{F}$$

then X is stochastically larger than Y and this means that

$$E[g(X)] \geq E[g(Y)]$$

for every increasing function g defined on $[0,\pi]$ (Marshall and Olkin (1979)). In particular, for the increasing function

$$g(\omega) = 1 - cos(\omega), \; 0 \leq \omega \leq \pi$$

we obtain,

$$1 - \int_0^\pi cos(\omega) d\tilde{F}_H(\omega) \geq 1 - \int_0^\pi cos(\omega) d\tilde{F}(\omega)$$

But this means that $\rho_1(H) \leq \rho_1$.

In the same way we can also prove the reversed inequality when the gain is monotone decreasing. □

Corollary 2. Suppose $\{Z_t\}$ is Gaussian. Then the simple expected HOC $\{E[D_j]\}$ from repeated differencing are monotone increasing,

$$E[D_j] \leq E[D_{j+1}], \; j = 1, 2, 3, \cdots. \tag{0.28}$$

and

$$\frac{\pi E[D_j]}{N-1} \longrightarrow \omega^* \tag{0.29}$$

where $\omega^* \leq \pi$ is the highest frequency in the spectral support.

Proof: (0.28) follows because of (0.2) and the fact that the squared gain of the difference operator is equal to

$$2(1 - cos(\omega))$$

and is seen to be increasing in $[0,\pi]$. Thus the simple expected HOC are monotone increasing. To prove (0.29) observe that the normalized expected HOC are also bounded:

$$0 \leq \frac{\pi E[D_j]}{N-1} \leq \pi$$

and therefore must converge. Also note that the spectral measure of $\{(\nabla^j Z)_t\}$, denoted by $\nu_j(\cdot)$, is given by

$$\nu_j(d\omega) = \frac{sin^{2j}(\omega/2) dF(\omega)}{\int_{-\pi}^{\pi} sin^{2j}(\lambda/2) dF(\lambda)}$$

where F is the spectral distribution function of $\{Z_t\}$. It follows that (0.2) can be written more compactly as

$$cos(\frac{\pi E[D_{j+1}]}{N-1}) = \int_{-\pi}^{\pi} cos(\omega)\nu_j(d\omega)$$

But from Kedem and Slud (1982) $\nu_j(\cdot)$ converges weakly,

$$\nu_j \Longrightarrow \frac{1}{2}\delta_{-\omega^*} + \frac{1}{2}\delta_{\omega^*},\ j \longrightarrow \infty$$

where δ_u is the unit point mass at u. Therefore as $j \longrightarrow \infty$

$$cos(\frac{\pi E[D_{j+1}]}{N-1}) \longrightarrow cos(\omega^*)$$

and use the fact that $cos(x),\ x \in [0, \pi]$ is monotone. □

Remark 1: A direct combinatorial way to obtain (0.28) is to note that for any strictly stationary process the inequality

$$\gamma(j) \leq \gamma(j+1) + \frac{1}{N}$$

always holds, and then letting $N \rightarrow \infty$. (0.28) follows because $\gamma(j)$ is independent of N.

A slightly more involved result gives a condition under which the first order correlation $\rho_1(\alpha)$, viewed as a function of $\alpha \in A \subset R^1$,

$$\rho_1 : A \longrightarrow [-1, 1]$$

is monotone.

Corollary 3. Consider the parametric family of filters $\{\mathcal{L}_\alpha(\cdot),\ \alpha \in A\}$, and assume that for each $\alpha \in A$, $\mathcal{L}_\alpha(\cdot)$ has a well defined inverse $\mathcal{L}^-{}_\alpha(\cdot)$. Suppose that for $\alpha \leq \beta,\ \alpha, \beta \in A$,

$$G(\omega; \alpha, \beta) = \frac{|H(\omega; \beta)|^2}{|H(\omega; \alpha)|^2}$$

is monotone decreasing in $\omega \in [0, \pi]$. Then

$$\rho_1(\alpha) \leq \rho_1(\beta)$$

If in addition $\{Z_t\}$ is Gaussian then also

$$E[D_\alpha] \geq E[D_\beta]$$

The inequalities are reversed when $G(\omega; \alpha, \beta)$ is monotone increasing in $\omega \in [0, \pi]$.

Proof: Operate on $\{Z_t(\alpha)\}$ with $\mathcal{L}_\beta \mathcal{L}^-{}_\alpha(\cdot)$. the squared gain of this sequential filter is $G(\omega; \alpha, \beta)$ which is assumed to be monotone decreasing. Therefore by Theorem 2 ,

$$\rho_1(\alpha) \leq \rho_1(G)$$

where $\rho_1(G)$ is the first order correlation in the filtered process

$$\mathcal{L}_\beta \mathcal{L}^-{}_\alpha \mathcal{L}_\alpha(Z)_t = \mathcal{L}_\beta(Z)_t = Z_t(\beta)$$

Therefore $\rho_1(G) = \rho_1(\beta)$ and

$$\rho_1(\alpha) \leq \rho_1(G) = \rho_1(\beta)$$

In the Gaussian case this entails,

$$\rho_1(\alpha) = cos(\frac{\pi E[D_\alpha]}{N-1}) \leq \rho_1(\beta) = cos(\frac{\pi E[D_\beta]}{N-1})$$

and since $cos(x)$ is monotone decreasing in $[0, \pi]$ we obtain

$$\frac{\pi E[D_\alpha]}{N-1} \geq \frac{\pi E[D_\beta]}{N-1}$$

The converse can be proved similarly.
□

0.4.2 Determining the correlation generating function from HOC

In this section we specialize to the parametric family

$$\mathcal{L}_\alpha(Z)_t = Z_t + \alpha Z_{t-1} + \alpha^2 Z_{t-2} + \cdots$$

The transfer function and squared gain are given by, respectively,

$$H(\omega;\alpha) = \frac{1}{1-\alpha\exp(-i\omega)}$$

and

$$|H(\omega;\alpha)|^2 = \frac{1}{1-2\alpha cos(\omega)+\alpha^2}$$

for $\omega \in [0,\pi], \alpha \in (-1,1)$. The corresponding impulse response is readily seen to be

$$h_n(\alpha) = \begin{cases} \alpha^n, & \text{n=0,1,2,}\cdots \\ 0, & \text{otherwise} \end{cases}$$

Therefore, from Lemma 2, the impulse response of $\mathcal{J}_\alpha(\cdot)$ is

$$g_n(\alpha) = \frac{\alpha^{|n|}}{1-\alpha^2},\ n = 0,\pm1,\pm2,\cdots$$

and by operating on ρ_k,

$$\mathcal{J}_\alpha(\rho)_n = \frac{\alpha^{|n|}}{1-\alpha^2} + \frac{1}{1-\alpha^2}\sum_{t=1}^{\infty}[\alpha^{|n+t|}+\alpha^{|n-t|}]\rho_t$$

Let $\phi(\alpha)$ be the correlation generating function of $\{Z_t\}$,

$$\phi(\alpha) \equiv \sum_{n=0}^{\infty}\rho_n\alpha^n,\ |\alpha|<1$$

It follows that,

$$\mathcal{J}_\alpha(\rho)_0 = \frac{1}{1-\alpha^2}[2\phi(\alpha)-1]$$

and

$$\mathcal{J}_\alpha(\rho)_1 = \frac{\alpha\phi(\alpha)+\alpha^{-1}\phi(\alpha)-\alpha^{-1}}{1-\alpha^2}$$

and therefore

$$\rho_1(\alpha) = \frac{(1+\alpha^2)\phi(\alpha) - 1}{\alpha[2\phi(\alpha) - 1]}, \ |\alpha| < 1 \tag{0.30}$$

Solving for $\phi(\alpha)$ in terms of $\rho_1(\alpha)$ we finally have,

Theorem 3. The correlation generating function $\phi(\alpha)$ of $\{Z_t\}$, a zero-mean stationary process, is obtained from $\rho_1(\alpha)$ by the equation

$$\phi(\alpha) = \frac{1 - \alpha\rho_1(\alpha)}{1 - 2\alpha\rho_1(\alpha) + \alpha^2}, \ |\alpha| < 1 \tag{0.31}$$

If in addition $\{Z_t\}$ is Gaussian, then

$$\phi(\alpha) = \frac{1 - \alpha cos(\pi\gamma(\alpha))}{1 - 2\alpha cos(\pi\gamma(\alpha)) + \alpha^2} = \frac{1 - \alpha cos(\pi\gamma(\alpha))}{|H(\pi\gamma(\alpha);\alpha)|^2}, \ |\alpha| < 1 \tag{0.32}$$

It follows from (0.32) that in the Gaussian case knowledge of the normalized expected zero-crossing rate $\gamma(\alpha)$ is equivalent to knowing the normalized spectral density

$$\tilde{f}(\omega) = \frac{f(\omega)}{\int_{-\pi}^{\pi} f(\lambda)d\lambda}$$

Corollary 4. Let $\{Z_t\}$, $t = 0, \pm 1, \pm 2, \cdots$, be a zero mean stationary Gaussian process. For $|\alpha| < 1$ and $\omega \in [0, \pi]$, the following equivalent relations hold:

$$\gamma(\alpha) \Longleftrightarrow \phi(\alpha) \Longleftrightarrow \rho_1(\alpha) \Longleftrightarrow \tilde{f}(\omega)$$

$\gamma(\alpha)$ is a new tool in time series analysis motivated by the equivalence relations in Corollary 4. The data example in the next section provides some insight necessary for judging the usefulness of this device. As examples, we consider some special cases.

Example 1: Gaussian white noise.
For $|\alpha| < 1$,

$$\rho_1(\alpha) = \alpha \tag{0.33}$$

$$\gamma(\alpha) = \frac{1}{\pi} cos^{-1}(\alpha) \tag{0.34}$$

and

$$\phi(\alpha) \equiv 1 \tag{0.35}$$

Given any process, we find it very helpful in applications to compare its zero-crossing rate $\gamma(\alpha)$ with that of white noise given in (0.34). See Figures 3,4.

Example 2: First order autoregressive process .
Consider a stationary Gaussian AR(1) process with parameter a_1,

$$Z_t = a_1 Z_{t-1} + \epsilon_t, \quad t = 0, \pm 1, \cdots$$

where $|a_1| < 1$, and $\{\epsilon_t\}$ is Gaussian white noise. For $|\alpha| < 1$,

$$\rho_1(\alpha) = \frac{\alpha + a_1}{1 + a_1 \alpha} \tag{0.36}$$

$$\gamma(\alpha) = \frac{1}{\pi} cos^{-1}\left(\frac{\alpha + a_1}{1 + a_1 \alpha}\right) \tag{0.37}$$

and

$$\phi(\alpha) = \frac{1}{1 - a_1 \alpha} \tag{0.38}$$

Figure 3 gives the graphs of $\gamma(\alpha)$ for $a_1 = -.6, \cdots, 0, \cdots, 0.6$. The case $a_1 = 0$ corresponds to white noise and is given for reference.

Example 3: Sum of sinusoids plus white noise.
Consider the mixed spectrum process (0.11). For $|\alpha| < 1$,

$$\rho_1(\alpha) = \frac{\sum_{j=1}^{p} \frac{\sigma_j^2 cos(\omega_j)}{1 - 2\alpha cos(\omega_j) + \alpha^2} + \frac{\alpha \sigma_\epsilon^2}{1-\alpha^2}}{\sum_{j=1}^{p} \frac{\sigma_j^2}{1 - 2\alpha cos(\omega_j) + \alpha^2} + \frac{\sigma_\epsilon^2}{1-\alpha^2}} \tag{0.39}$$

$$\gamma(\alpha) = \frac{1}{\pi} cos^{-1}(\rho_1(\alpha)) \tag{0.40}$$

and

$$\phi(\alpha) = \frac{\sum_{j=1}^{p} \frac{\sigma_j^2(1-\alpha cos(\omega_j))}{1-2\alpha cos(\omega_j)+\alpha^2} + \sigma_\epsilon^2}{\sum_{j=1}^{p} \sigma_j^2 + \sigma_\epsilon^2} \tag{0.41}$$

Figure 4 gives the graphs of $\gamma(\alpha)$ in the case of $p = 1$ for several values of the frequency ω_1 when the signal to noise ratio is 20dB (very little noise). The figure also gives the zero-crossing rate of white noise for comparison. Near the origin the graph of $\gamma(\alpha)$ is close to a horizontal line as is expected in light of our next result.

As a function of $\alpha \in (-1, 1)$, $\gamma(\alpha)$ is *always* monotone decreasing, a fact that makes it useful in comparing different processes. When the process is a pure sinusoid, $\gamma(\alpha)$ is a constant. In the Gaussian case the converse is also true.

Theorem 4. Let $\{Z_t\}$, $t = 0, \pm 1, \pm 2, \cdots$, be a zero mean stationary Gaussian process. Then

(a) $\gamma(\alpha)$ is monotone decreasing in $\alpha \in (-1, 1)$.
(b) $\gamma(\alpha)$ is constant if and only if $\{Z_t\}$ a pure sinusoid with probability one.

Proof: To prove (a) we apply Corollary 3 to

$$|H(\omega; \alpha)|^2 = \frac{1}{1 - 2\alpha cos(\omega) + \alpha^2}$$

We show that for $-1 < \alpha \le \beta < 1$

$$G(\omega; \alpha, \beta) = \frac{|H(\omega; \beta)|^2}{|H(\omega; \alpha)|^2} = \frac{1 - 2\alpha cos(\omega) + \alpha^2}{1 - 2\beta cos(\omega) + \beta^2}$$

is monotone decreasing. So, for $0 \le \omega_1 \le \omega_2 \le \pi$ the numerator of the difference

$$G(\omega_2; \alpha, \beta) - G(\omega_1; \alpha, \beta)$$

is equal to

$$2(cos(\omega_1) - cos(\omega_2))(1 - \alpha\beta)(\alpha - \beta) \leq 0$$

and (a) follows.

To prove (b), if $\{Z_t\}$ is a pure sinusoid with frequency ω_1, then from (0.39),

$$\rho_1(\alpha) = cos(\omega_1) = cos(\pi\gamma(\alpha))$$

or for all $|\alpha| < 1$,

$$\gamma(\alpha) = \frac{\omega_1}{\pi}$$

and $\gamma(\alpha)$ is constant on $(-1, 1)$. Conversely, if $\gamma(\alpha)$ is constant for all $\alpha \in (-1, 1)$, then there exists $\omega_1 \in [0, \pi]$ such that

$$\gamma(\alpha) = \frac{\omega_1}{\pi}$$

for all $\alpha \in (-1, 1)$. Thus, from (0.32) we have,

$$\phi(\alpha) = \frac{1 - \alpha cos(\pi\gamma(\alpha))}{1 - 2\alpha cos(\pi\gamma(\alpha)) + \alpha^2} = \frac{1 - \alpha cos(\omega_1)}{1 - 2\alpha cos(\omega_1) + \alpha^2}$$

But this is the correlation generating function of a pure sinusoid. To complete the proof, note that

$$\rho_1 = \phi'(0) = cos(\omega_1) \qquad \rho_2 = \frac{1}{2}\phi''(0) = cos(2\omega_1)$$

Therefore,

$$\frac{1}{Var[Z_t]}E[Z_t - 2\rho_1 Z_{t-1} + Z_{t-2}]^2 = 2(1 - 2\rho_1^2 + \rho_2) = 0$$

so that with probability one $\{Z_t\}$ satisfies the stochastic difference equation

$$Z_t - 2\rho_1 Z_{t-1} + Z_{t-2} = 0$$

whose solution is a sinusoid with frequency ω_1.

□

Remark 2. We can improve statement (b) in Theorem 4 by noting that if for some $\alpha_1, \alpha_2 \in (-1, 1)$,

$$\gamma(\alpha_1) = \gamma(\alpha_2), \; -1 < \alpha_1 < 0 < \alpha_2 < 1 \tag{0.42}$$

then by monotonicity $\gamma(\alpha)$ is constant in the interval $[\alpha_1, \alpha_2]$ that contains the origin. Because $\phi(\alpha)$ is analytic at $\alpha = 0$, the same argument as in the above proof shows that $\{Z_t\}$ must then be a sinusoid under this weaker condition. Thus (b) can be replaced by the stronger statement that $\{Z_t\}$ is a pure sinusoid with probability one if and only if (0.42) holds for some $-1 < \alpha_1 < 0 < \alpha_2 < 1$. Compare with Kedem(1984).

Figure 3. Graphs of $\gamma(\alpha)$ from AR(1) with parameter $a_1 = -0.6, -0.5, \cdots, 0, 0.1, \cdots, 0.6$. $a_1 = 0$ corresponds to white noise.

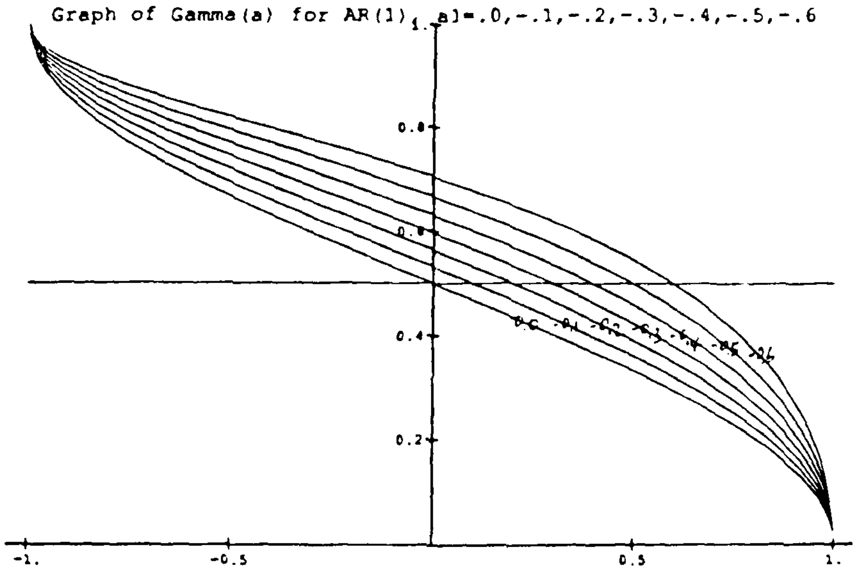

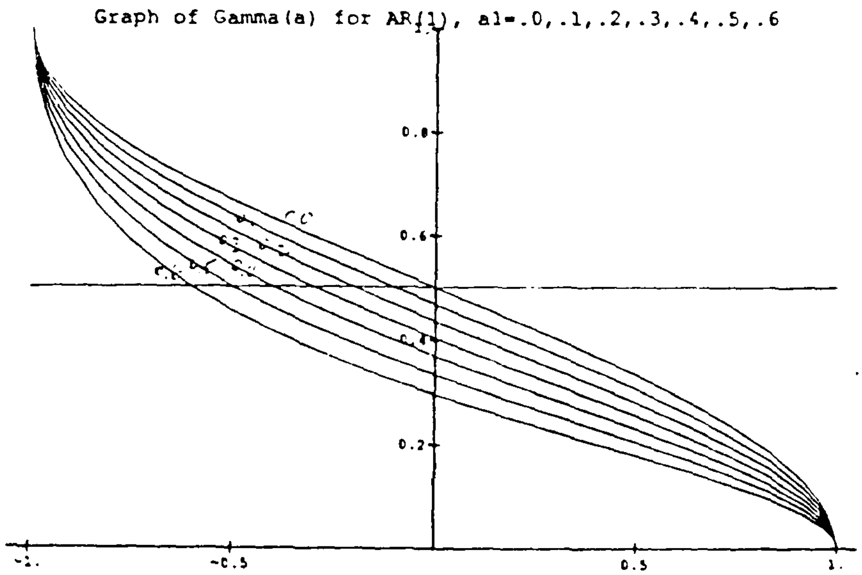

Figure 4. Plots of $\gamma(\alpha)$ from a single sinusoid plus white noise; SNR=20dB. The plots correspond to frequency $\omega_1 = 0.05\pi, 0.15\pi, \cdots, 0.95\pi$. The intersecting curve is the zero-crossing rate of white noise.

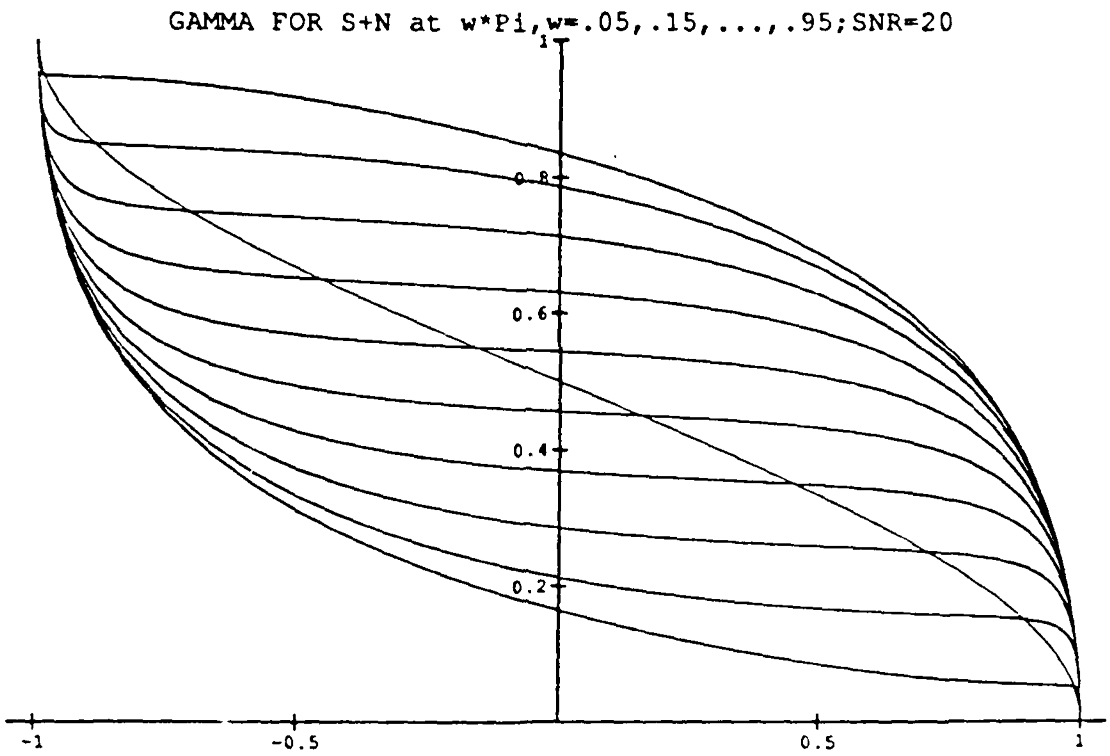

0.5 $\gamma_N(\theta)$ as a descriptive-diagnostic tool

Given a parametric family of filters $\{\mathcal{L}_\theta(\cdot)\}$, there are several ways to apply the corresponding observed zero-crossing rate $\gamma_N(\theta)$. We describe two procedures and then apply them to real data.

0.5.1 Two useful procedures

(A). HOC-plots.
In this procedure, $\gamma_N(\theta)$ is plotted as a function of $\theta \in \Theta$ as a descriptive device that summarizes the data very much like the estimated spectral density.

When $\mathcal{L}_\theta(\cdot) = \nabla^{\theta-1}$, then for sufficiently large N, $\gamma_N(\theta)$ is increasing as a function of $\theta = 1, 2, \cdots$. Experience shows that the initial rate of increase is a useful discriminator.

When $\mathcal{L}_\alpha = \sum_{j=0}^{\infty} \alpha^j \mathcal{B}^j$, $\gamma_N(\alpha)$ tends to decrease for $\alpha \in (-1, 1)$. From the Gaussian case we already know that attention should be given to $\gamma_N(\alpha)$ for α-values near the origin.

In any application, it is helpful to include also the plot of $\gamma(\theta)$ from a ***known*** process, usually Gaussian white noise, for reference as done in Figures 1,2.

If a certain hypothesis is entertained, we can test it by observing whether the HOC plot from the data falls within certain probability bands. The probability limits can be obtained from the asymptotic normality of $\gamma_N(\theta)$ when it holds. A surprisingly good approximation to the variance of $\gamma_N(\theta)$ under the Gaussian assumption is given for each fixed θ by the formula (Kedem(1987)):

$$Var[\gamma_N(\theta)] \approx \tag{0.43}$$

$$\frac{\gamma(\theta)(1-\gamma(\theta))}{N-1} + [1 - \frac{V(\theta)}{N-1}]\frac{2\gamma(\theta)(1-\gamma(\theta))(\nu(\theta)-\gamma(\theta))}{(1-\nu(\theta))(N-1)}$$

where

$$V(\theta) = [\frac{1-\gamma(\theta)}{1-\nu(\theta)}][1-(\frac{\nu(\theta)-\gamma(\theta)}{1-\gamma(\theta)})^{N-1}] \tag{0.44}$$

$$\nu(\theta) = \frac{1-2\lambda_1(\theta)+\lambda_2(\theta)}{2(1-\lambda_1(\theta))} \tag{0.45}$$

and

$$\lambda_n(\theta) = \frac{1}{2} + \frac{1}{\pi} sin^{-1} \rho_n(\theta),\ n = 1, 2, \cdots \tag{0.46}$$

Observe that $\gamma(\theta) = 1 - \lambda_1(\theta)$. In this connection we have.

Theorem 5. Assume that $\{Z_t\}$ is Gaussian white noise and consider $\gamma_N(\alpha)$ from the α-filter. Then for each fixed $\alpha \in (-1, 1)$ as $N \longrightarrow \infty$,

$$\frac{\gamma_N(\alpha) - \gamma(\alpha)}{\sqrt{Var[\gamma_N(\alpha)]}} \longrightarrow_{\mathcal{L}} \mathcal{N}(0,1)$$

Proof: Follows easily by noting that $\{Z_t\}$ is Gaussian, D_α is a sum of indicators, and that $\rho_n(\alpha) = \alpha^{|n|}, n = 0, \pm 1, \cdots$.

□

Thus, under the hypothesis of Gaussian white noise, for each fixed $\alpha \in (-1, 1)$ we can find an approximate probability interval that contains $\gamma_N(\alpha)$ using (0.43).

(B). Deviation from white noise.

Measuring the deviation of the *observed* HOC from the *expected* HOC of Gaussian white noise, is a recommended procedure. A successful application of this idea has been reported in Dickstein et al.(1989) in discriminating between ultrasound echo signatures obtained from bonded aluminum specimens that underwent different surface treatment prior to bonding. To measure deviation from white noise, Dickstein et al. used the ψ^2 statistic discussed in Kedem and Slud(1982), but using observed rather than expected HOC from white noise.

Another variation, is to construct HOC-grams from

$$\gamma_N(\theta) - \gamma_W(\theta),\ \theta \in \Theta \tag{0.47}$$

where $\gamma_W(\theta)$ is the expected zero-crossing rate of Gaussian white noise. By applying (0.47) to different stretches of the data each of length N, we obtaine an image in two-dimensional *time* $\times\ \Theta$ space called *HOC-gram*. When the α-filter is used, the HOC-grams are obtained from

$$\gamma_N(\alpha) - \frac{1}{\pi}cos^{-1}(\alpha),\ \alpha \in (-1,1) \tag{0.48}$$

Many other variations are possible.

0.5.2 Tracking the vocal sound of a humpback whale

The vocal sound of cetaceans is a subject of interest to marine biologists who consider the sound of these animals as a feature of their adaptation to aquatic existence (Schevill and Watkins (1962).) Tracking and identification of distinctive whistle patterns of whales and porpoises is thus an important element of the research on cetaceans. The actual business of recording sound at sea presents some difficulties because of ambient sea noise due in part to machinary on board ships and to the movement of waves against bodies such as ship hulls. In what follows we apply HOC analysis to a vocal sound series uttered by a humpback whale in ambient sea noise. The series was recorded 45 miles east of Boston. More information about the series and the recording device can be found in Schevill and Watkins (1962).

The series consists of 3 seconds worth of data sampled at the rate of 20 KHz, and recorded with 12 bit resolution in the form of integers in the range 0 – 4095. Because we are interested in tracking as well as identification, the data were partitioned into stretches of 0.1 second containing 2048 observations each.

Figure 5 was obtained from the stretch of data ending at 0.2 seconds. The figure shows plots of the observed zero-crossing rate $\gamma_N(\theta)$ from simple HOC and HOC from the α- filter. As explained above, the figure contains also 95% probability limits and $\gamma(\theta)$ from Gaussian white noise for reference and for measuring the similarity to white noise. Observe that $\gamma(\theta)$ is between the probability limits by construction. The hypothesis of white noise is obviously rejected, as is well expected, by both types of HOC, but the HOC from the α-filter are more informative because they point to the possibility that the data may follow a low-order AR process. This is seen by comparison with Figure 3. It is interesting to note that the simple observed HOC behave very much like the expected simple HOC from white noise for higher differences, while the observed HOC from the α-filter exhibit a similar phenomenon for values of α, roughly, greater than 0.4. That is to say, in this sense some parts of HOC-plots are more informative than others.

Figure 6 portrays the same analysis applied to the stretch of data ending with 0.5 seconds. The data now show greater similarity to white noise as seen from both HOC plots (a),(b), but the hypothesis of white noise is still rejected. We conclude that the signal is less powerful than the previous one.

Figure 7 shows a marked deviation from white noise and the presence of a powerful signal in the stretch of data ending at 1.4 seconds. The signal is not sinusoidal because with that much power we would expect from the simple HOC that $\gamma_N(1) \approx \gamma_N(2)$. But since this obviously is not the case, a sinusoidal component is ruled out. However, by comparing the HOC-plot corresponding to the α-filter with the HOC-plots in Figure 3 we see that a low-order AR sound component is a very reasonable model for this stretch of data. *This example shows that the HOC plots from the α-filter and from repeated differencing complement each other. Both are useful in applications.*

Next we obtain the HOC-grams (0.48)

$$\gamma_N(\alpha) - \frac{1}{\pi} cos^{-1}(\alpha), \ \alpha \in (-1, 1)$$

for 19 α-values, $\alpha = -0.9, -0.8, \cdots, 0, 0.1, \cdots, 0.9$, and for non-overlaping stretches of data each corresponding to 0.1 seconds. The α-values are on the ordinate while the abscissa is the time axis. The values of the HOC-gram are given in the form of grey levels. Darker levels correspond to more negative values of $\gamma_N(\alpha) - \frac{1}{\pi} cos^{-1}(\alpha)$, while lighter levels correspond to more positive values. We can see from the HOC-gram given in Figure 8 that the entire data set contains three distinct pronounced utterances. From Schevill and Watkins (1962) we know that this is what was in fact expected.

It is interesting to see what a spectral-gram from the same stretches of data gives. Figure 9 gives the logspectral- gram obtained from AR-spectral estimates by fitting to each subseries of 0.1 seconds an AR(20) model. It is possible to see correspondence between the HOC-gram and the logspectral-gram, but the HOC-gram gives a much clearer tracking of the vocal sound series.

Figure 5. Plots of $\gamma_N(\theta)$ and 95% probability limits for the stretch of whale data ending at 0.2 seconds. (a) Simple HOC. (b) HOC from the α-filter.

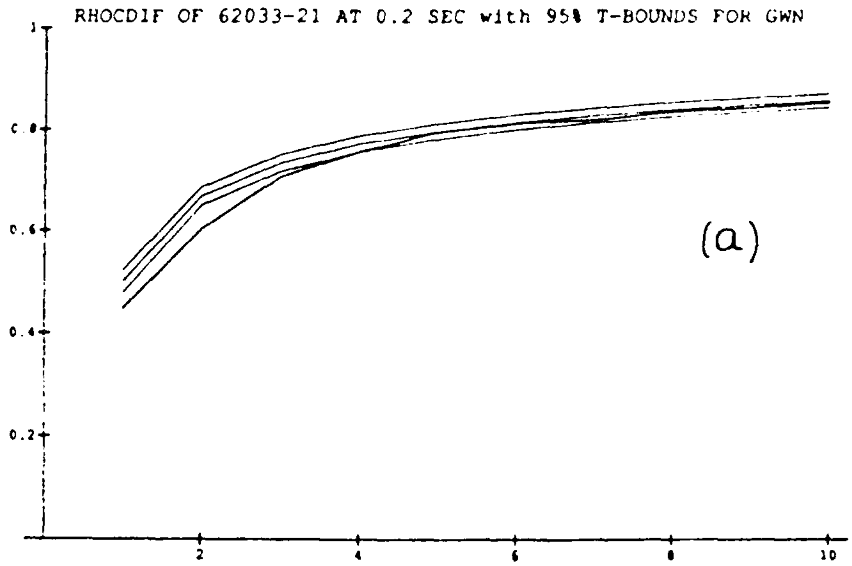

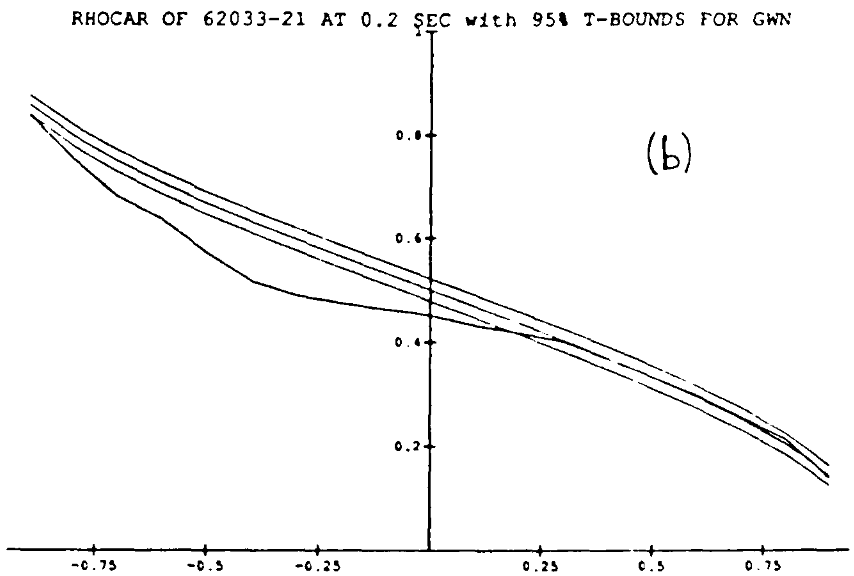

Figure 6. Plots of $\gamma_N(\theta)$ and 95% probability limits for the stretch of whale data ending at 0.5 seconds. (a) Simple HOC. (b) HOC from the α-filter.

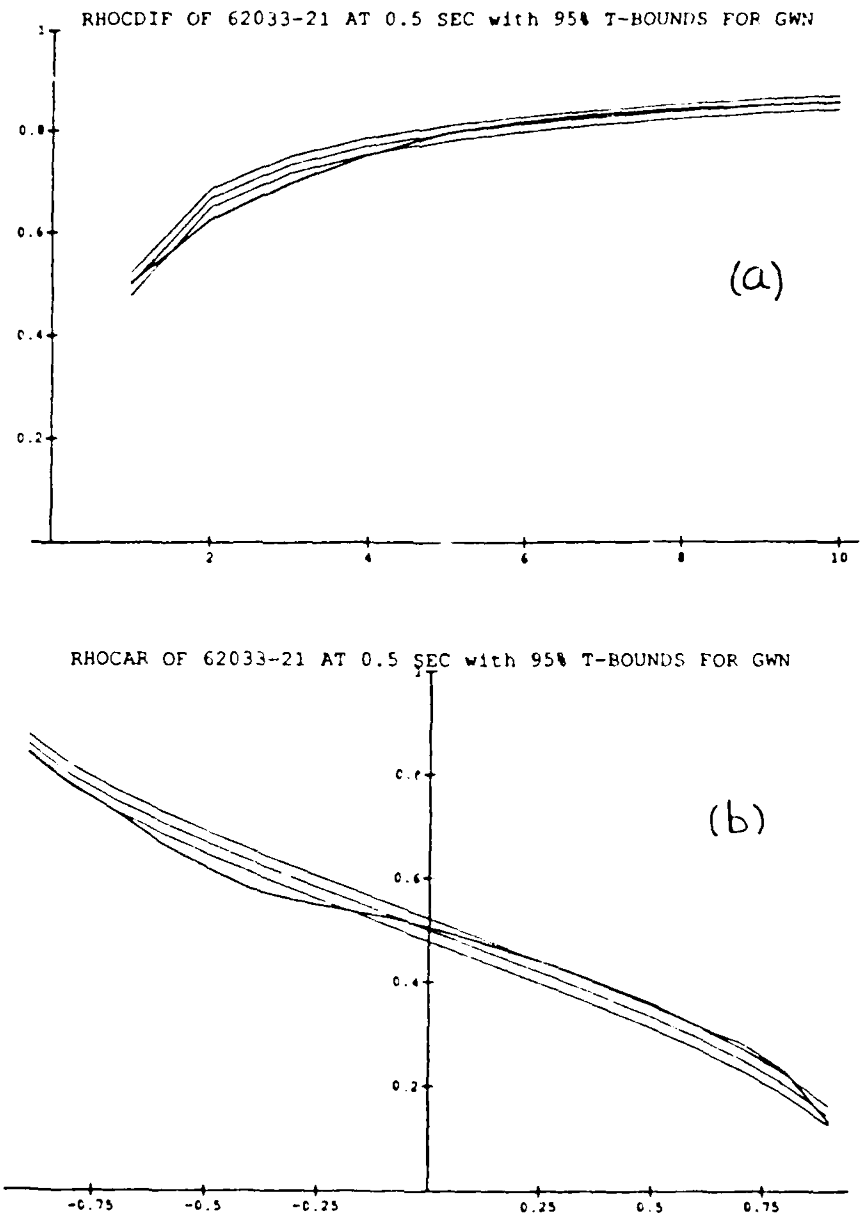

Figure 7. Plots of $\gamma_N(\theta)$ and 95% probability limits for the stretch of whale data ending at 1.4 seconds. (a) Simple HOC. (b) HOC from the α-filter.

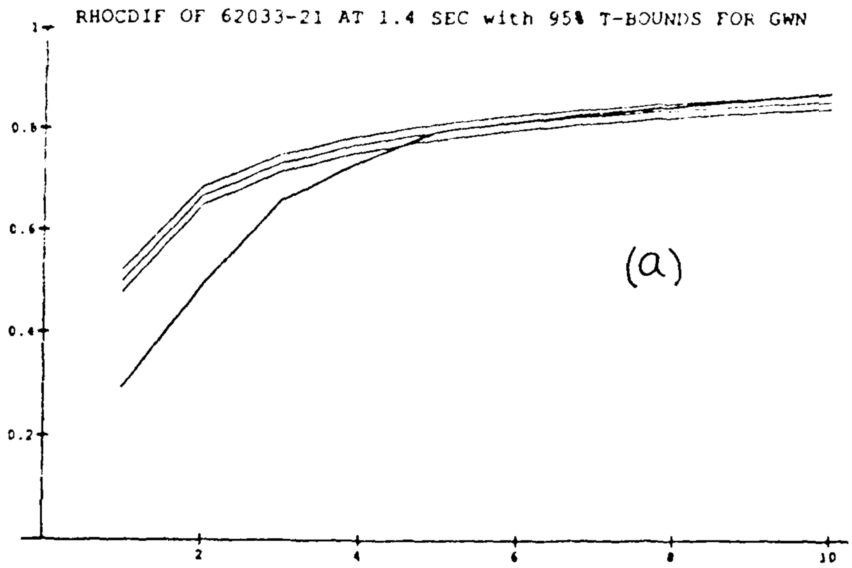

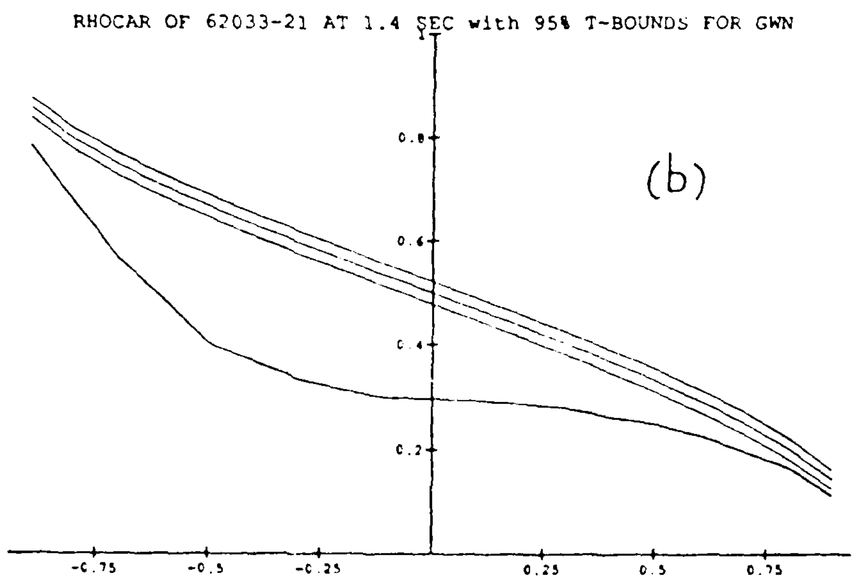

Figure 8. HOC-gram from a vocal sound of a humpback whale.

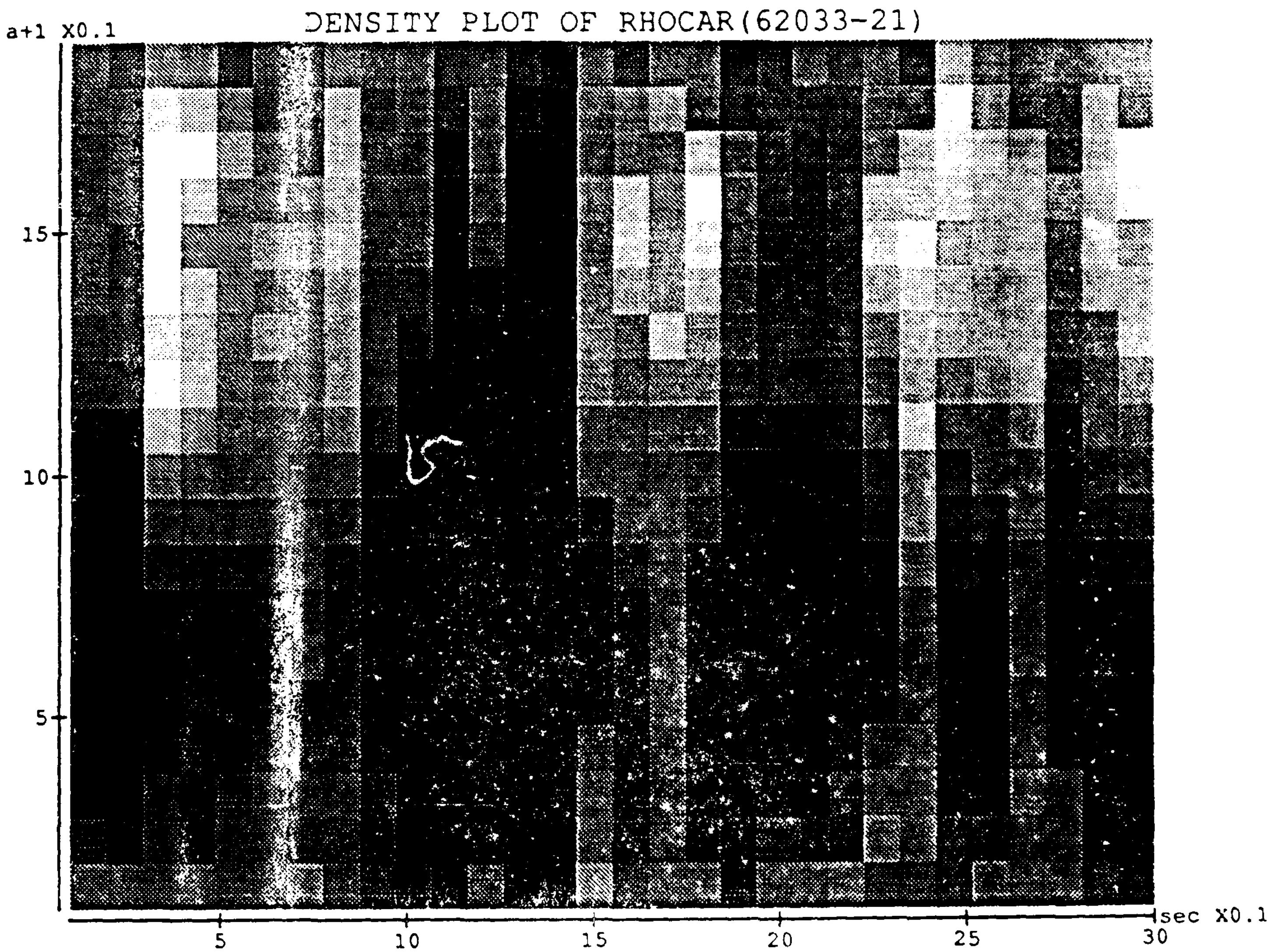

Figure 9. logspectral-gram from a vocal sound of a humpback whale.

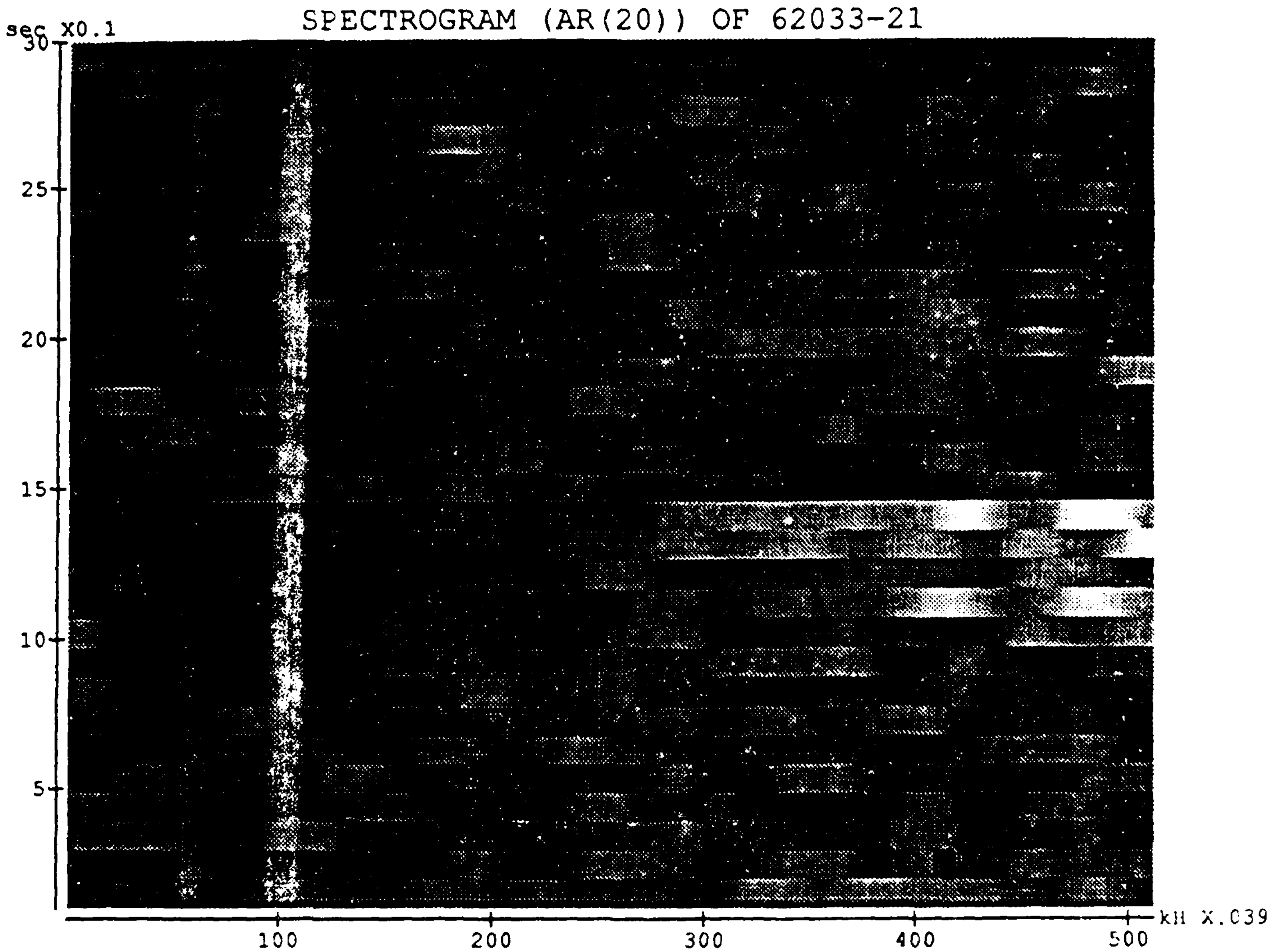

REFERENCES

1. David, F.N.(1953). A note on the evaluation of the multivariate normal integral. *Biometrika*, 40, 458-459.

2. Dickstein, P., Y. Segal, E. Segal, and A.N. Sinclair (1989). Statistical pattern recognition techniques: A sample problem of ultrasonic determination of interfacial weakness in adhesive joints. *Jour. of Nondestructive Evaluation*.8.

3. He, S. and Kedem (1989a). Higher order crossings spectral analysis of an almost periodic random sequence in noise. *IEEE Tr. Infor. Theory*, 35, 360-370.

4. ——————(1989b). The zero-crossing rate of autoregressive processes and its link to unit roots. To appear in *Jour. of Time Series.*

5. ——————(1988). On the stieltjes-Sheppard orthant probability formula. Submitted.

6. Kedem, B. (1984). On the sinusoidal limit of stationary time series. *Annals of Stat.*, 12, 665-674.

7. ———(1986). Spectral analysis and discrimination by zero-crossings. *IEEE Proceedings*, 74, 1477-1493.

8. ———(1987). Higher order crossings in time series model identification. *Technometrics*, 19, 193-204.

9. ——— and E. Slud (1982). Time series discrimination by higher order crossings. Annals of Stat., 10, 786-794.

10. Marshall, A. and I. Olkin (1979), *Inequalities: Theory of Mjorization and Its Applications*, Academic Press, New York.

11. Schevill, W.E., and W.A. Watkins (1962). *Whale and Porpoise Voices*, Woods Hole Oceanographic Institution, Woods Hole, Massachusetts.

Captions of Figures and Tables

Figure 1. Realizations from processes with adjoined random variables with p=0.1, 0.25, 0.5, 0.75.

Figure 2. Plots of normalized HOC. (a) Simple HOC. (b) HOC from the α-filter.

Figure 3. Graphs of $\gamma(\alpha)$ from AR(1) with parameter $a_1 = -0.6, -0.5, \cdots, 0, 0.1, \cdots, 0.6$. $a_1 = 0$ corresponds to white noise.

Figure 4. Plots of $\gamma(\alpha)$ from a single sinusoid plus white noise; SNR=20dB. The plots correspond to frequency $\omega_1 = 0.05\pi, 0.15\pi, \cdots, 0.95\pi$. The intersecting curve is the zero-crossing rate of white noise.

Figure 5. Plots of $\gamma_N(\theta)$ and 95% probability limits for the stretch of whale data ending at 0.2 seconds. (a) Simple HOC. (b) HOC from the α-filter.

Figure 6. Plots of $\gamma_N(\theta)$ and 95% probability limits for the stretch of whale data ending at 0.5 seconds. (a) Simple HOC. (b) HOC from the α-filter.

Figure 7. Plots of $\gamma_N(\theta)$ and 95% probability limits for the stretch of whale data ending at 1.4 seconds. (a) Simple HOC. (b) HOC from the α-filter.

Figure 8. HOC-gram from a vocal sound of a humpback whale.

Figure 9. logspectral-gram from a vocal sound of a humpback whale.

Table 1. Convergence of $\frac{\pi D_{a_1}}{N-1}$ towards $\omega_1 = 0.8$ with $N = 10000$ where the signal to noise ratio (SNR) is given in dB.